Multi-decadal projections of surface and interior pathways of the Fukushima Cesium-137 radioactive plume

Vincent Rossi, Erik van Sebille, Alexander Sen Gupta, Véronique Garçon, Matthew England

Multi-decadal projections of surface and interior pathways of the Fukushima Cesium-137 radioactive plume

Vincent Rossi[a1], Erik Van Sebille[b], Alex Sen Gupta[b], Véronique Garçon[c], Matthew H. England[b].

[a] IFISC (Institute for Cross-Disciplinary Physics and Complex Systems), CSIC-UIB, Palma de Mallorca, Spain.

[b] University of New South Wales, Climate Change Research Center & ARC Centre of Excellence for Climate System Science, Sydney 2052, Australia.

[c] Laboratoire d'Etude en Géophysique et Océanographie Spatiales, CNRS/UPS/IRD/CNES, 14 av. E.Belin, Toulouse 31400, France.

[1]Corresponding author: Vincent Rossi, vincent.rossi.ocean@gmail.com, +34 971 172 915.

Highlights

- Cs-137 plume strongly diluted by July 2011, reaches American coast by 2013/2014
- Mode water formation and persistent upwelling affect Cs-137 concentrations
- Cs-137 enters the deep ocean and exits the North Pacific in the next 30 years

Abstract:

Following the March 2011 Fukushima disaster, large amounts of water contaminated with radionuclides, including Cesium-137, were released into the Pacific Ocean. With a half-life of 30.1 years, Cs-137 has the potential to travel large distances within the ocean. Using an ensemble of regional eddy-resolving simulations, this study investigates the long-term ventilation pathways of the leaked Cs-137 in the North Pacific Ocean. The simulations suggest that the contaminated plume would have been rapidly diluted below 10,000 Bq/m^3 by the energetic Kuroshio Current and Kurushio Extension by July 2011. Based on our source function which constitute the upper range of the published estimate to date, waters with Cs-137 concentrations > 10 Bq/m^3 are projected to reach the northwestern American coast and the Hawaiian archipelago by early 2014. Driven by quasi-zonal oceanic jets, shelf waters north of 45°N experience Cs-137 levels of 10-30 Bq/m^3 between 2014-2020, while the Californian coast is projected to see lower concentrations (10-20 Bq/m^3) slightly later (2016-2025). This late but prolonged exposure is related to subsurface pathways of mode waters, where Cs-137 is subducted toward the subtropics before being upwelled from deeper sources along the southern Californian coast. The model projects that Fukushima-derived Cs-137 will penetrate the interior ocean and spread to other oceanic basins over the next two decades and beyond. Our simulated results are extensively discussed regarding the numerous uncertainties related to the neglected processes, to the source function and to large-scale variability.

Keywords: Radioactive tracers; North Pacific; Ocean circulation; Mode water formation; Fukushima nuclear disaster; 3D Lagrangian modeling.

Introduction:

The Tohoku earthquake and the associated tsunami on 11 March 2011 caused enormous human losses and infrastructure damage. It also triggered a nuclear disaster in which the Fukushima Daiichi nuclear plant released large amounts of radionuclides into the atmosphere and ocean [Buesseler et al., 2011; Chino et al., 2011; Stohl et al., 2011], including Cesium-137 (Cs-137). Recent studies suggest that the Fukushima disaster caused the largest-ever direct release of anthropogenic radionuclides into the ocean [Bailly du Bois et al., 2012]. Although several attempts have been made to quantify the total amount of Cs-137 released [Buesseler et al., 2012 and references therein], considerable uncertainty remains related to the duration and intensity of release. Early reports found a strong impact of the contaminated water on local marine life [Garnier-Laplace et al., 2011], while a recent study performed off Japan suggested that radiation risks due to Cs isotopes had dropped below the levels generally considered harmful to marine animals and humans within three months of the accident [Buesseler et al., 2012]. However, the poorly known long-term effects of these radionuclides on marine biota [Garnier-Laplace et al., 2011] combined with the unknown factors relating to the magnitude of release and the redistribution of Cs-137 via oceanic circulation prevent a robust assessment of the potential impacts. Behrens et al [2012] have studied the evolution of the Cs-137 plume in the North Pacific for the first decade following the release using passive tracer calculations in the NEMO ocean circulation model. Very recently, Nakano and Povinec, [2012] used a coarse resolution model (2˚) with climatological forcing to study the long-term dispersal of the radioactive plume. Here, we use Lagrangian particles within the high resolution Ocean General Circulation Model For the Earth Simulator (OFES) to focus on multi-decadal (up to 30 years) evolution, confirming some of the results reported by Behrens et al [2012] and Nakano and Povinec, [2012] and analyzing further the surface and sub-surface pathways for an extended period of time.

Cs-137 is of purely anthropogenic origin and is released into the atmosphere and the ocean via nuclear weapons testing, nuclear plants releases, nuclear accidents, and the dumping of radioactive wastes. Even though Cs-137 has only been present in the environment for about six decades, it has already penetrated to the deep ocean [Livingston and Povinec, 2000]. Background oceanic concentrations vary between 10^{-4} to 10^{-1} Bq/m^3 in the southern hemisphere to a maximum of a few Bq/m^3 in the North Pacific [Aoyama et al., 2011]. Since Cs-137 behaves as a passive tracer in seawater and has a 30.1 years half-life, it can aptly be used to study the decadal-scale circulation pathways and ventilation time-scales of water masses in the global ocean [Aoyama et al., 2011 and references therein]. Hence, the future distribution of Fukushima-derived Cs-137 in the ocean provides an opportunity to validate oceanic numerical models and their parameters over decadal time-scales [Dietze and Kriest, 2011], provided the source function can be tightly constrained.

Here, we focus our analysis on the simulated long-term and large-scale evolution of Cs-137 in the North Pacific as a result of the Fukushima radioactive incident, without re-evaluating the initial near-coastal sub-annual spreading, neither the release scenario, as it has been pursued in previous studies [Buesseler et al., 2012; Kawamura et al., 2011; Tsumune et al., 2012; Estournel et al., 2012]. Using an ensemble member mean distribution from 27 Lagrangian regional simulations, the aim of this study is to estimate the dilution and spreading pathways of the Cs-137 radioactive plume in the North Pacific over the next few decades. In addition we examine the location, timing and concentrations of Cs-137 contaminated waters reaching selected coastal areas in the North Pacific. The vertical evolution of the Cs-137 tracer is also analyzed along specific sections across the basin providing a full three dimensional analysis of the decadal pathways.

Methods:

To simulate the spatial evolution of Cs-137 in the North Pacific Ocean, we advect a large number of neutrally buoyant Lagrangian particles from a region off Fukushima using 3D velocities from a global Oceanic Global Circulation Model. The Lagrangian technique has been shown to be well suited to problems in which high contaminant gradients are involved, since spurious numerical diffusion is not introduced [Nakano et al., 2010; Monte et al., 2009]. Cs-137 is considered as a conservative dissolved tracer as scavenging, sedimentation, re-suspension from the sediment, biological uptake (or bioaccumulation) and food-chain transfer (or biomagnification) are negligible. This assumption is supported by laboratory studies that demonstrate this inert behavior [Vogel et al., 2010; IAEA, 2004; Heldal et al., 2001].

Given the large uncertainties involved in atmospheric transport patterns and estimates of total release, atmospheric deposition at the ocean surface has not been taken into account here [Buesseler et al., 2012; Stohl et al., 2011; Yasunari et al., 2011]. Similarly, river inputs and background pre-Fukushima concentrations of Cs-137 have been neglected, with initial concentrations set to zero. The simulations thus only incorporate the material newly released into seawater from the Fukushima disaster (see also the discussion section).

The numerical model used to derive the Lagrangian advection fields is the Ocean model For the Earth Simulator (OFES) based on the MOM3 ocean model [Masumoto et al., 2004; Sasaki et al., 2008]. OFES is initialized from the World Ocean Atlas 1998 climatological fields, and then run for 57 years using NCEP forcing. It is an eddy-resolving global ocean model with a horizontal resolution of 1/10 degree and 54 vertical layers. The fine resolution of the Lagrangian Cs-137 simulations is a key feature of this study since mesoscale eddies have considerable importance in the transport of Cs-137 [Behrens et al., 2012; Tsumune et al., 2011]. Furthermore, the OFES model has been comprehensively assessed in the Kuroshio region and the Northern Pacific: the outputs used here (taken from years 1980 to 2006) have been shown to adequately capture the seasonal, interannual and multi-decadal variability of

126 the surface and sub-surface circulation in this region [Taguchi et al., 2010; 2007; Nonaka et
127 al., 2012; Sasaki et al., 2012]. They have also been widely used and validated for mode water
128 formation and subduction rate in the North Pacific [Aoki et al. 2007; Qu and Chen, 2009] as
129 well as for larger-scale thermohaline circulation [Van Sebille et al. 2011].
130 In our approach, the Lagrangian particle concentrations can be scaled to a Cs-137
131 concentration that gives an estimate of the total quantity of tracer introduced from
132 Fukushima, as done in an Eulerian study by Hazell and England [2003]. Both approaches
133 have the advantage of being adaptable to any new estimates of total release and allows for
134 comparison with future *in-situ* measurements when adding background oceanic
135 concentrations. Latest estimates suggest a major release of 22 (± 12) PBq of Cs-137 over one
136 month starting mid-March [Bailly du Bois et al., 2012]. Although some regional studies
137 estimates lower amounts [Tsumune et al., 2012; Estournel et al., 2012], an analysis based on
138 both *in-situ* data and numerical simulations confirmed that the source term used here (22 PBq
139 over one month, see also discussion section) is the most probable one [Buesseler et al., 2012].
140 To simulate the release of waters contaminated with dissolved Cs-137, an ensemble of
141 experiments is performed, in each of which a total of 100,000 passive Lagrangian particles
142 are released from March 13 to April 13. Specifically, we release 10,000 particles at the
143 surface ocean off the Fukushima plant every three days over this month, i.e. during the first
144 month following the Fukushima disaster. A non-local source function is used by choosing
145 randomly the spatial location of release of each particle from a two-dimensional Gaussian
146 distribution that is centered on the location of the Fukushima plant and has a decay length-
147 scale of 30 km, mimicking the mixing effect of non-resolved near-coastal currents [Behrens
148 et al., 2012]. In order to assess the sensitivity of the tracer evolution to the initial oceanic
149 conditions, an ensemble of 27 release experiments is performed, each simulation starting in a
150 different year (from 1980 to 2006).

151 Particles are advected with a 4th order Runge-Kutta integration scheme, based on a new
152 version of the toolset described in Paris et al. [2013], for 30 years using 3-day snapshots of
153 OFES velocity data for the North Pacific region. As is typical in these kinds of multi-decadal
154 basin-scale Lagrangian experiments in eddy-resolving models, there is no need for an
155 additional random walk term, as mesoscale eddy variability accounts for an effective
156 horizontal and vertical diffusion of the particles (see also sect. Discussion).
157 In order to integrate the particles trajectories for a 30-year period, velocity fields are looped,
158 so that after 2006 the integration continues using the 1980 fields. Similarly to what was done
159 in Van Sebille et al., [2012], we tested the impact of looping the velocity field in this way by
160 comparing a standard looped simulation (i.e. from 1980 to 2006 and back) with a short loop
161 simulation (1980 to 1990, looped over these 10 years), and no significant difference in the
162 tracer evolution was found (not shown). While the simulations project forward in time by
163 three decades based on the circulation fields of 1980-2006, the variability across the
164 ensemble set gives a measure of uncertainty into the future under the assumption that ocean
165 circulation variability over the next few decades will not be substantially different from that
166 seen over the past few decades. This is a reasonable assumption given that over this time
167 period changes in circulation related to natural variability are likely to dominate over any
168 potential changes driven by global warming (e.g. [Hawkins and Sutton, 2009]). The
169 integration of a particle is stopped when it leaves the North Pacific domain (0-60°N and
170 120°E -100°W). Rather than adjusting the scaling of the radioactivity carried by the particles
171 over time, we have chosen here to simulate the natural radioactive decay of the Cs-137
172 isotope by randomly removing particles over time with a probability corresponding to a half-
173 life of 30.1 years. This allows for an interpretation of the set of particles as a subsample of the
174 Cs-137 atoms, and keeps us clear from the issue of mixing that is inherent in the

interpretation where each particle is a finite-size water mass (see also p. 66 of Van Sebille [2009]).

Throughout this study, we present the 27-member ensemble-mean distribution (i.e. corresponding to a total of 27 * 100 000 Lagrangian trajectories) and highlight the robust pathways associated with the ocean circulation. Where applicable, an examination of the spread in the distributions provides information on the sensitivity of the pathways and time-scales to interannual variations of the circulation.

Results:

Surface pathways through the North Pacific:

Figure 1 shows snapshots of Cs-137 concentrations at different times in the surface ocean (0 - 200 m averages) and the corresponding concentrations along 37.5°N (which approximates the core of the eastward plume of Cs-137). Along the zonal section (Fig. 1e), the spread in concentrations associated with different ensemble members is relatively small (less than 10% of the concentrations reported in Fig. 1e). This suggests that at large scales, the pathways are relatively insensitive to the initial ocean conditions and interannual-decadal variability in the circulation. Indeed, a recent modeling study by Behrens et al., [2012] found that the impact of the initial ocean condition would largely fade after the first 2-3 years. As such, the lack of real-time circulation fields during the initial release is unlikely to significantly affect our results on interannual time-scales and beyond.

The plume is quickly advected away almost zonally from Japan due to the vigorous Kuroshio Current and Kuroshio Extension as it passes over the Izu-Ogasawara Ridge (~ 142°E). Within this pathway there is a rapid dilution of Cs-137 with time. Concentrations fall below 10,000 Bq/m^3 everywhere by the end of July 2011, from a maximum concentration of about 150,000 Bq/m^3 near the Japanese coast at the end of March 2011, in good agreement with coastal

studies [Buesseler et al., 2011; Tsumune et al., 2012]. Most of this decay is related to the intense eddy field of the Kuroshio Current and Kuroshio Extension that leads to strong horizontal and vertical mixing. Further east, the Kuroshio Extension encounters successive topographic features such as the Shatsky Rise (160°E) and the Emperor Seamounts (170°E), which have been associated with meandering of the main flow [Niiler et al., 2003]. It then rejoins the interior gyre circulation as the North Pacific Current (NPC), which advects the plume eastward towards the coast of North America. The NPC is not a uniform eastward flow but is punctuated by zonal fronts where intensified flow occurs at relatively stable latitudes, despite strong seasonal and interannual variations in forcing [e.g. Oka and Kiu, 2011]. The strong eastward transport at 45°N in April 2012 (Fig. 1a) might correspond to a quasi-stationary jet associated with the Polar Front, sometimes coinciding with the Subarctic front [Oka and Kiu, 2011]. Further south, an intensified eastward advection is also visible at ~ 32.5°N, at the location of the Kuroshio Extension jet [Qiu and Chen, 2005]. Note that although most of the surface plume is contained in the subpolar gyre, Cs-137 is gradually transported into the subtropical gyre probably due to the mesoscale activity of the Kuroshio Extension jet and to the Ekman transport under westerly winds (Fig. 1a, b). After reaching the American continental margin around April 2014 at 45°N, the ensemble-mean of the contaminated water plume then splits into two branches. One branch flows northwards to feed the Alaska Current, thereby entraining part of the contaminated waters into the Subarctic Gyre. The other branch flows southwards feeding the California Current. South of 40°N, the offshore Ekman drift at the coast associated with coastal upwelling helps to prevent Cs-137 enriched surface waters from directly reaching the coast. The persistent upwelling off California forced by the prevailing northeasterly winds maintains Cs-137-contaminated waters slightly offshore the shelf for up to 5 years after release (Fig. 1b, c).

In the western Pacific, the North Equatorial Current recirculates Cs-137 enriched water back westward at around 30°N (Fig. 1b). After 10 years (Fig. 1d) contaminated surface waters have been diluted almost everywhere to concentrations below 10 Bq/m^3, with a noticeable local maximum in the surface Eastern Subtropical North Pacific (15-35°N, 135-120°W). When the westward-flowing North Equatorial Current enters the Philippines Sea, the long-term pathways become more complex. Part of the water flows northward and re-enters the Kuroshio Current again, closing the recirculation of contaminated water within the subtropical gyre. Much of the remainder moves southwest and exits the model domain. This occurs as water is entrained into the southward-flowing Mindanao Current south of 15°N, and then either through the Celebes Sea to feed the Indonesian Throughflow, or toward the Equator to enter the South Pacific via the Equatorial Undercurrent [Nakano et al., 2010]. Another alternative route is via the South China Sea north of 15°N and then via the Indonesian Throughflow to reach the Indian Ocean. In Aoyama et al. [2011], a core of high concentration Cs-137 was found in the eastern part of the Indian Ocean which was believed to have travelled via the Indonesian Throughflow after originating in the Pacific region 10 to 20 years earlier by atmospheric deposition in the 1970s. Evaluating the relative importance of these exit routes is beyond the scope of this study but may constitute an important pathway of contaminated water over the next few decades.

After 30 years (in 2041) about 25% of the total initial Cs-137 released remains within the North Pacific gyre, 25% has left the gyre, and the remaining 50% has of course disappeared by natural radioactive decay. Of the amount that left the North Pacific, a very small fraction has been lost northward toward the Bering Sea, with the largest part injected into the southern hemisphere through the different routes discussed above and in [Tsumune et al., 2011; Nakano et al., 2010].

Intrusion of the plume onto coastal areas of the Eastern North Pacific:

To investigate the penetration of contaminated water onto the North American shelf, Cs-137 concentrations (0-200 m) in a coastal band parallel to the coastline are examined. Note that the intra-ensemble spread for the selected latitudes is small (up to 20% in Fig. 2b), attesting of the robustness of our long-term estimations. The first waters characterized by Cs-137 levels above 1 Bq/m^3 are projected to reach the US west coast at around 45°N in mid-2013, while rapidly increasing up to 5 Bq/m^3 from early 2014 (Fig. 2a, b). Maximum concentrations between 20 and 30 Bq/m^3 occur from mid-2014 (3 years after the initial release) to mid-2018 off Oregon/British Columbia (45 to 55°N), in good agreement with the simulations by Behrens et al., [2012]. Cs-137 concentrations above 10 Bq/m^3 in surface shelf waters near Vancouver (49°N) are modeled from 2014 to mid-2021, i.e. over ~ 6 years. The early and strong rise in Cs-137 concentrations seems related to the Subarctic/Polar front jet that rapidly advects waters toward the shelf [Oka and Qiu, 2010]. The first Cs-137 contaminated waters start to reach the Californian coast from mid-2014, with local maxima at 28-32°N (Baja California/San Diego) and 35-40°N (Northern California). Maximum concentrations are lower than in the north, ranging from 10 to 20 Bq/m^3, due to longer transit times associated to larger dilution and natural radioactive decay. Concentrations above 10 Bq/m^3 near the Californian coast occur from 2016, some 2 years after the northern coast (Fig. 2b), as coastal divergence in the Californian upwelling prevents contaminated surface waters from reaching the coast. While the maximum concentrations off California are weaker than those north of 40°N, elevated Cs-137 concentrations remain evident from 2016 until around 2025, about 3 years longer than along the northern coastline (Fig. 2a). While the northern areas are mostly affected by the first impact of the plume, the southern areas experience prolonged input probably due to the persistent upwelling of contaminated waters that originate from the subsurface.

In the centre of the North Pacific, the evolution of the Cs-137 plume evolution is studied by averaging surface concentrations over the area 18-23°N and 160-155°W, covering all islands of the Hawaiian Archipelago (Fig. 2b). Slightly contaminated waters start to reach the area by 2013, but Cs-137 concentrations above 5 Bq/m^3 only arrive in early 2015 and remain above this concentration until early 2025. Maximum concentrations of about 8 Bq/m^3 occur from mid-2017 to mid-2021. The archipelago is not situated along the main pathway of the plume and so is only affected by water that recirculates or mixes southward (Fig. 1a-c).

Vertical distribution of Cs-137 and interior pathways:

As the contaminated water spreads laterally across the North Pacific basin, there is also substantial vertical transport (Fig. 3-6). By 2016 (Fig. 3), i.e. 5 years after the initial release, about 42 % of total remaining Cs-137 is at depths of 200-600 m, with 5% at greater depths (600-1500 m). By 2031, Cs-137 has penetrated to considerable depth with only about 28 % of the remaining Cs-137 in surface layers, 48 % in central water masses (200-600 m depth) and 22 % within intermediate waters (600-1500 m depth), indicating that Fukushima derived Cs-137 is likely to be found in Mode and Intermediate Waters in the future. However, because there is no significant Deep-Water formation in the North Pacific, only a very small proportion, less than 3 %, penetrates deeper than 1500 m by the year 2030.

Diapycnal mixing and vertical water mass movements, for example within late winter pycnostads, are likely to be the main factors driving the deep intrusion of Fukushima derived Cs-137, favored by the period of release; namely, at the end of winter when mixed layers in the North Pacific are relatively deep (up to 200-300 m). Using a Cs-137 labeled water mass analysis, Aoyama et al. [2008] showed that Central Mode Waters and North Pacific Subtropical Mode Waters are formed by subduction of surface waters in the subarctic regions of the western North Pacific before being transported into the ocean interior to lower

299 latitudes. On the western side of the basin, the model simulates intense subduction and
300 vertical mixing of Cs-137 enriched waters already within the first 2-4 years of release (2013-
301 2014). The subduction area extends from 30-45°N / 145°E-160°W (Fig. 4a) and reaches to
302 depths of ~ 1000 m (Fig. 4b). This appears to be associated with the formation of three
303 distinct water masses: Denser Central Mode Water, Lighter Central Mode Water and
304 Subtropical Mode Water, as documented by Oka and Qiu, [2011]. The southernmost (25-
305 30°N) region of subduction, related to the North Pacific Subtropical Mode Water formation
306 (σ_0 ~ 25 kg/m^3), is not likely to entrain elevated Cs-137 waters, since the Fukushima release
307 occurred further north. However, subduction of both Denser (σ_0 ~ 27 kg/m^3 within 37.5-
308 45°N) and Lighter (σ_0 ~ 26 kg/m^3 within 30-37.5°N) Central Mode Waters (Fig. 4a) must
309 entrain high Cs-137 concentrations into the deep ocean [Oka and Qiu, 2011; Aoyama et al.,
310 2008]. This is also evidenced by the asymmetrical bowl shape structure along 165°E (Fig. 4c)
311 that can be compared to the Cs-137 profile from *in-situ* data collected in 2002 by Aoyama et
312 al., [2008] (their Fig. 1). These observed spatial patterns are well reproduced by the model,
313 suggesting that the mechanisms driving the elevated deep concentrations are realistically
314 simulated. Although the meridional slope of the stratification appears almost symmetrical
315 north and south of 30°N, Cs-137 penetrates down to ~ 1000 m between 30-45°N (Lighter and
316 Denser Central Mode Water) but only down to ~ 400 m between 20-30°N (North Pacific
317 Subtropical Mode Waters), possibly due to the Kuroshio and Kuroshio Extension that act as
318 barriers to the southward penetration of the tracer [Behrens et al., 2012].
319 Further east and in April 2014, the two regions of elevated levels of Cs-137 (20 to 60 Bq/m^3)
320 centered at 32°N and 45°N (Fig. 4d at 140°W) correspond to the two zonal jets mentioned
321 above, flowing toward North America and extending down to 400 m and 500 m respectively.
322 In early 2014 at 30°N (Fig. 4b), the coastal upwelling along the Californian coast is clear and
323 prevents the surface plume from penetrating onto the shelf. By early 2021, relatively high

Cs-137 concentrations (~10 Bq/m^3) are found between 400-600 m in the east, spreading south of 40°N (20-40°N / 180°E-120°W; Fig. 5a). These mode waters were subducted in the western North Pacific along the main pathway of the plume about 6 to 9 years earlier and have gradually been upwelled along isopycnals while moving eastward. The mean depth of the 26 kg/m^3 isopycnal (black contours on Fig. 4, 5) reveals the zonal tilting of the stratification in the eastern half of the North Pacific basin. Lighter Central Mode Waters, and Subtropical Mode Waters in moderate proportion, were formed between 300-600 m in the west (Fig. 4a, b, c) and are then uplifted to 150-250 m to the southeast of the basin (Fig. 5a). When these mode waters approach the continental shelf, it leads to higher subsurface (150-250 m) concentrations off the south California upwelling region in 2021 (south of 35°N; Fig. 5b, c).

Although these specific 3 dimensional pathways below and above ~ 40˚N might solely explain why the shelf regions of North America are affected differently depending on latitude by the radioactive plume (Fig. 2a), local processes might also play a role. When investigating the vertical circulation at two extreme locations, representing the southern and northern shelf regions of the Californian Upwelling system, we found a marked difference in the mean origin of upwelled waters. Source waters of upwelling along the northern shelves are somehow shallower (~ 50-150 m) than along the southern areas (~ 100-250 m; Fig. 6), primarily due to a lower offshore Ekman transport [Rossi et al. 2009]. Therefore, due to a combination of remote and local effects, Cs-137 enriched mode waters upwelled by Ekman pumping intrude onto the Southern US shelves over a longer period of time (~ 9 years, Fig. 2a, b) than over the Northern US shelves.

Discussion:

Long-term evolution of the Cs-137 plume:

Using an ensemble of Lagrangian particle simulations, this study has examined the likely future pathways and concentration levels of Cs-137 in the North Pacific resulting from the 2011 Fukushima nuclear disaster. Given the considerable uncertainties in all the source terms, our approach considers only the direct oceanic source but remains adaptable to any future improved estimates of the source function. In addition, the OFES velocity field used here is currently the most realistic eddy-resolving resolution of the North Pacific circulation, thus providing reasonable confidence in our predictions of the long-term fate of the Fukushima Cs-137. The Kuroshio Current, Kuroshio Extension and their associated mesoscale activity causes a rapid dilution and offshore transport of contaminated waters, with maximum concentrations dropping by an order of magnitude or more within the first 4 months, in good agreement with Buesseler et al. [2012]. Our model suggests that the first Fukushima derived Cs-137 contaminated waters (> 1 Bq/m^3) are expected to reach Hawaii and the North American shelf in early 2014. A very recent study (Kamenik et al. [2013) indicated that the radiation plume has not been detected up to September 2012 at the main Hawaiian Islands, in very good agreement with our simulated results (Fig. 2b), independently of the source function used, providing more confidence in our "ensemble" approach and the velocity field used. On the eastern boundary of the North Pacific, Cs-137 levels ranging between 5 and 30 Bq/m^3 are found along the coastline and remain elevated for 5 to 10 years depending on latitude. The highest Cs-137 concentrations (10-30 Bq/m^3) are simulated along the northwest American continental shelf (north of 40°N) from early 2014, persisting for about 6 years. In contrast, maximum concentrations are projected to be lower (10-20 Bq/m^3) from 2016 along the Californian coast, but these can be expected to prevail for a longer period of time (~ 9 years). This seems to be due to the subduction of Cs-137 enriched mode waters along the path of the plume in the western North Pacific, which is subsequently upwelled from below the thermocline along the south Californian upwelling. These transit-times across the Pacific

(3 to 5 years after release) are consistent with the results of Nakano and Povinec, [2012] which indicated that the plume will reach US west coast about 4-5 years after the accident. It is however 1-2 years earlier than that estimated by Behrens et al., [2012], probably due to the different velocity field they used. Our simulations suggest that Cs-137 will penetrate mode and intermediate waters over the next 30 years, in line with the results of Behrens et al., [2012] and Nakano and Povinec, [2012]. Overall, our modeled pathways in the first 10 years are in good agreement with the findings of Behrens et al., [2012], although they used a different source function. Note that some differences remain in the simulated concentrations and timing. For example, Moreover, the time taken for the plume to reach the Hawaiian Archipelago (~ 3-5 years) is very similar in both studies, while Cs-137 concentrations simulated by Behrens et al., [2012] are about half that in our projections, which might be essentially due to the lower source function retained in their study (10 PBq). Our simulated long-term pathways revealed some differences (such as the strength of the southern recirculation and the absence of small-scale jets in their simulations) with the results of Nakano and Povinec, [2012] likely to be due to the coarse resolution (2˚) and the climatological velocity field they used. It is further noted that while Behrens et al. [2012] focus mainly on the vertically integrated tracer inventory projected over the next 10 years and, here we have assessed both surface and interior pathways for the next two decades using high resolution model outputs.

Finally, our simulations suggest that after 30 years about 25% of the initial Cs-137 release is likely to exit the North Pacific toward other oceanic basins, with most exiting via the Indonesian Throughflow and/or crossing the Equator to join the South Pacific; only a small proportion leaves via the Bering Strait into the Arctic, a pathway also simulated by Behrens et al., [2012]. This finding is consistent with the analysis of interbasin transport of the previously released Cs-137 undertaken by Tsumune et al. [2011], who find that the North

399 Pacific has been a source of Cs-137 to other ocean basins, in particular via the Indonesian
400 Archipelago toward the Indian Ocean. It is also in line with the global simulations performed
401 by Nakano and Povinec, [2012] which indicate that the Fukushima-derived Cs-137 will be
402 transported to the South Pacific and the Indian Ocean after 20 years.
403
404 *Neglected processes and uncertainties:*
405 A number of assumptions are made in the present analysis that could affect the evolution of
406 oceanic Cs-137. In this multi-decadal basin-scale Lagrangian experiments using an eddy-
407 resolving model, we have assumed that there is no need for an additional random walk term
408 as mesoscale eddy variability accounts for an effective horizontal and vertical diffusion of the
409 particles. When comparing one member of the ensemble ran with artificial vertical and
410 horizontal diffusion to the original member without random walk, we confirmed that the
411 effect on Cs-137 concentrations in the core of the plume is relatively small (~ 20 %). In
412 contrast, a larger impact was observed on the southern flank of the plume, suggesting an
413 enhancement of the southern recirculation loop, especially from year 1 onward. Note
414 however that this effect concerned low Cs-137 concentrations (< 10 $Bq.m^{-3}$) and that our
415 results take into account part of this diffusion effect by considering the 27 members of the
416 ensemble of simulations.
417 Another simplification is to simulate Cs-137 as a passive conservative (apart of its
418 radioactive decay) tracer. Alternative modeling approaches which consider the interactions of
419 dissolved nucleotide with the solid phase do exist and imply that the suspended matter
420 equation, the settling of particles and the deposition/erosion of the bottom sediment have to
421 be modeled (e.g. Periañez, [2000]; Periañez and Elliot, [2002]; Kobayashi et al. [2007]; Choi
422 et al. [2013]). By neglecting scavenging and associated settling/deposition processes, our
423 surface estimates might be slightly overestimated while the deep penetration of Cs-137 might

424 be slightly underestimated. The portion of Cs-137 released to the open ocean versus the
425 amount of radioactive material deposited into the sediment near the coast (up to 10% or less
426 of the total release) is relatively sensitive to local conditions such as vertical mixing and
427 dispersion [Choi et al. 2013]. Note however that scavenging and sediment
428 deposition/resuspension processes are likely to be much more important in coastal regions
429 than in the oligotrophic gyre of the North Pacific due to the low concentrations of particulate
430 matter and the distance to the seabed.
431 We have also neglected land/ocean interactions, in particular inputs of contaminated water
432 from rivers and groundwater. Although rivers have been transported additional Cs-137 into
433 the ocean, especially during heavy rain events [Nagao et al., 2013], the total estimate of these
434 source terms remains unknown. In addition, rivers are unlikely to make up more than a small
435 contribution to dissolved Cs-137 in the open ocean as the isotopes bind to soil particles
436 [Tsumune et al., 2011]. A recent study by Kusakabe et al. [2013] showed that the Cs-137
437 distribution in coastal sediments is not directly linked to the proximity with river mouths and
438 with the site of the accident, but it seems rather driven by the concentration of the overlying
439 water during the first few months after the accident and by the physical characteristics of the
440 sediment.
441 A larger source of uncertainty relates to the atmospheric fallout onto the surface ocean. Most
442 of the airborne Cs-137 released from Fukushima is thought to have been deposited over the
443 North Pacific Ocean due to the prevailing westerly winds during March-April 2011 [Stohl et
444 al., 2011; Yasunari et al., 2011], which would lead to higher levels of Cs-137 in surface
445 waters than those calculated here. Buesseler et al. [2012] found that the most consistent
446 atmospheric fallout over the Pacific Ocean matches the highest total atmospheric emission
447 available (estimates range from about 9.9 to 35.8 PBq, see Table S2 of Buesseler et al.
448 [2012]). Indeed, Stohl et al. [2011] showed that about 80 % of the total 35.8 PBq (23.3 - 50.1

PBq) were deposited over the Pacific Ocean, although the timing and the detailed extension of the deposition remains unclear. Another estimate by Kawamura et al. [2011], also used by Nakano and Povinec, [2012], suggest that 5 PBq, over the total 13 PBq atmospheric release, deposited over the North-West Pacific Ocean. If a significant proportion of the atmospheric deposition occurred in the area of mode water formation (30-45°N, 140-170°E), this would lead to an increase of the Cs-137 penetration into the deep ocean, due to subsequent subduction during late winter/early spring [Oka and Qiu, 2011]. In addition, the choice of a non-local input area (using a circle of diameter 60 km) might somehow partly capture the effect of the atmospheric deposition in the immediate vicinity of Fukushima [Behrens et al., 2012]. However, since the estimates derived from modeling studies are highly variable and due to a lack of *in-situ* measurements [Tsumune et al. 2013], it is difficult to constrain the pattern and magnitude of the atmospheric fallout. In addition, a recent large-scale study [Nakano and Povinec, 2012] confirmed that due to a large dispersion surface, direct radionuclide deposition on surface waters of the North Pacific has only a small effect (~ 10%) on the long-term assessment of the plume.

Concerning the oceanic source, the latest estimates of total Cs-137 directly release in the ocean range from ~1 PBq to 27 PBq from measured radioactivities [Japanese Government, 2011; Kawamura et al., 2011; Bailly-du-Bois et al., 2012; Normile, 2013; Tsumune et al. 2013] and from 3.5 to 5.9 PBq as estimated from numerical simulations and inverse methods [Tsumune et al., 2012; 2013; Estournel et al., 2012]. Here we assumed a release of 22 PBq injected over 1 month (mid-March to mid-April) as the most reliable estimate [Buesseler et al., 2012]. An additional simulation was also performed using a modified total release of 27 PBq, with ~ 80% (22 PBq) released during the first month and the remaining ~ 20 % (5 PBq) during the next 3 months, based on the total estimates of Bailly du Bois et al. [2012]. Apart from linearly scaling up the Cs-137 concentrations reported here by ~ 20%, the results for

this ensemble of experiments are qualitatively identical in the long-term (not shown). For the decadal time-scales considered here, the total release is of much more importance than its precise timing within the first couple of months after the disaster. Another recent study estimated the Cs-137 released over the first three months directly into the coastal ocean liying between 5.1 and 5.5 PBq, while emphasizing that uncertainties remain on the amount of radionuclides released during the first few days after the accident [Estournel et al., 2012]. If further studies confirmed that this lower source is the most reliable one, the concentrations reported here could be roughly multiplied by a factor 0.25 to obtain more realistic estimates. Aoyama et al. [2013] reports lately that the surface Cs-137 plume was transported along 40˚N with concentrations greater than 10 $Bq.m^{-3}$ reaching the international date line in March 2012, i.e. one year after the accident. Although a perfect matching between small-scale *in-situ* observations and our large-scale simulated concentrations is not expected, one way to take into account this observational constraint is to find the scaling factor that would make our results match with these observations. We have thus extracted the Cs-137 concentrations along the International Date Line (averaged within a 2 degrees band from 179˚E to 179˚W) and we investigated the time-series at 40˚N. To match our simulated concentrations with the observed localized concentrations, a scaling factor of 0.15 is used and could also provide an updated inverse estimate of the total release amount of 3.3 PBq. This is consistent with the latest estimates of total Cs-137 release ranging from ~1 PBq to 27 PBq (Normile, [2013]; Tsumune et al. [2013]), indicating a potential overestimation of the source function by Bailly-du-Bois et al. [2012]. If a total release of 3.3 PBq is confirmed, the coastal areas north of 45˚N will be the only shelf regions affected by Cs-137 concentrations of ~ 10 $Bq.m^{-3}$ in late 2014 - early 2015, while other southern shelf regions and the Hawaiian archipelago will see low concentrations (< 5 $Bq.m^{-3}$) from 2017 onward.

Given that a large proportion of the multi-decadal variability of the North Pacific circulation is associated with the Pacific Decadal Oscillation (PDO), we have performed additional simulations to test "artificially" the effect of extreme PDO state on the Cs-137 plume. This effect was tested by looping over 30 years OFES velocities during a period dominated by positive PDO (1983-1987) to compare to an experiment looping velocities over a period dominated by negative PDO (1998-2002). The main discrepancies are related to (i) the north/south orientation of the axis of the Kuroshio Current (KC) and Kuroshio Extension (KE), (ii) the zonal transport of the KC/KE and associated jets and (iii) the strength of the southern recirculation. Indeed, Qiu [2000, 2003] already described the inter-annual variability of the Kuroshio system identifying two different states. On one hand the elongated state, which has been associated with a negative PDO, is characterized by a strong mean zonal transport and increased jet-like structure of the KC/KE accompanied with a more intense southern recirculation. On the other hand, a weaker zonal advection (contracted state), a more southward axis of the KC and KE and a weaker recirculation have been associated with positive PDO phases [Qiu, 2000; 2003; Oka et al. 2012]. It is however difficult to predict the impact of these processes on the long-term advection of the plume within the vast North Pacific because they are highly space and time dependent. Specifically, the PDO variability is remotely forced by large scale wind stress curl forcing in the central North Pacific [Qiu 2003; Taguchi et al. 2007] and it then takes some time for the resulting SSH and thermocline depth anomalies to propagate toward the area off Japan. In addition, this inter-decadal variability has been also shown to influence the eddy-activity of the region, with opposite effects found for both upstream and downstream region of the Kuroshio system [Oka et al. 2012]. They also revealed complex interactions with the mode water formation in the NW Pacific that will affect the future 3 dimensional pathways of the plume but that are impossible to anticipate presently.

Overall, our estimates of net Cs-137 released into the ocean are on the conservative side, in terms of total quantity and duration, when considering all sources and mechanisms involved. In addition, two very recent publications suggest that the release of nucleotides in the ocean might have been longer than just 1-2 months after the Fukushima accident [Kanda, 2013; Normile, 2013], supporting further our choice of a "scalable" approach due to the large uncertainties remaining on the source function.

Conclusions:

Based on output from an eddy-resolving ocean model we find that the Fukushima Cs-137 plume is rapidly diluted within the Kuroshio system over a time-scale of 4 months. Over the subsequent few decades the model projects that a significant amount of Fukushima-derived nucleotides will spread across the North-Pacific basin, driven primarily by advection within the subtropical gyre. The model estimates that a component will be injected into the interior ocean via subduction before eventually returning to the surface by coastal upwelling along the west coast of North America. Ultimately the signature will spread into other ocean basins, particularly the Indian and South Pacific Oceans. The long-term evolution of the modeled plume, eventually scaled up to a reliable source function, could be compared to observations from future monitoring programs to evaluate water mass pathways and transit times in the North Pacific.

Acknowledgements:

The OFES simulation was conducted on the Earth Simulator under the support of JAMSTEC. E.V.S. and M.H.E. are supported by the Australian Research Council. The authors thank the three anonymous reviewers for their constructive comments that substantially improved the manuscript.

548

549 **References:**

550 Aoki, S., M. Hariyama, H. Mitsudera, H. Sasaki, and Y. Sasai, 2007. Formation regions of
551 Subantarctic Mode Water detected by OFES and Argo profiling floats, Geophys. Res. Lett.,
552 34 (10), L10606, doi:10.1029/2007GL029828.

553 Aoyama, M., K. Hirose, K. Nemoto, Y. Takatsuki and D. Tsumune, 2008. Water masses
554 labeled with global fallout 137Cs formed by subduction in the North Pacific, Geophys. Res.
555 Lett., 35, L01604.

556 Aoyama M., P. P. Povinec, J-A. Sanchez-Cabeza, 2011. The Southern Hemisphere Ocean
557 Tracer Studies (SHOTS) project. Prog. Oceanogr., 89, 1-6.

558 Bailly du Bois P., P. Laguionie, D. Boust, I. Korsakissok, D. Didier and B. Fiévet, 2012.
559 Estimation of marine source-term following Fukushima Dai-ichi accident, J. Environ.
560 Radioactiv. 114, 2–9.

561 Behrens, E., F.U. Schwarzkopf, J.F. Lübbecke and C.W. Böning, 2012. Model simulations on
562 the long-term dispersal of 137Cs released into the Pacific Ocean off Fukushima. Environ.
563 Res. Lett., 7, 034004.

564 Buesseler, K., M. Aoyama, and M. Fukasawa, 2011. Impacts of the Fukushima Nuclear
565 Power Plants on Marine Radioactivity, Environ. Sci. Technol., 45, 9931-9935.

566 Buesseler, K.O., S.R. Jayne, N.S. Fisher, I.I. Rypina, H. Baumann, Z. Baumann, C.F. Breiera,
567 E.M. Douglass, J. George, A.M. Macdonald, H. Miyamoto, J. Nishikawa, S.M. Pike, and S.
568 Yoshida, 2012. Fukushima-derived radionuclides in the ocean and biota off Japan, Proc. Natl.
569 Acad. Sci. USA, 10.1073/pnas.1120794109.

570 Chino, M., H. Nakayama, H. Nagai, H. Terada, G. Katata and H. Yamazawa, 2011.
571 Preliminary estimation of release amounts of 131I and 137Cs accidentally discharged from

572 the Fukushima Daiichi nuclear power plant into the atmosphere, J. Nucl. Sci. Technol., 48,
573 1129-1134.

574 Choi, Y., S. Kida, and K. Takahasi, 2013. The impact of oceanic circulation and phase
575 transfer on the dispersion of radionuclides released from the Fukushima Dai-ichi Nuclear
576 Power Plant, Biogeosciences Discuss., 10, 3677-3705.

577 Dietze H. and I. Kriest, 2011. Tracer distribution in the Pacific Ocean following a release off
578 Japan – what does an oceanic general circulation model tell us? Ocean Sci. Discuss., 8, 1441-
579 1466.

580 Estournel, C., E. Bosc, M. Bocquet, C. Ulses, P. Marsaleix, V. Winiarek, I. Osvath, C.
581 Nguyen, T. Duhaut, F. Lyard, H. Michaud and F. Auclair, 2012. Assessment of the amount of
582 cesium-137 released into the Pacific Ocean after the Fukushima accident and analysis of its
583 dispersion in Japanese coastal waters, J. Geophys. Res., 117, C11014,
584 doi:10.1029/2012JC007933.

585 Garnier-Laplace, J., K. Beaugelin-Seiller and T.G. Hinton, 2011. Fukushima wildlife dose
586 reconstruction signals ecological consequences. Environ. Sci. Technol., 45, 5077-5078.

587 Hazell D.R. and M.H. England, 2003. Prediction of the fate of radioactive material in the
588 South Pacific Ocean using a global high resolution ocean model, J. Environ. Radioactiv., 65,
589 329-355.

590 Hawkins, E., and R. Sutton, 2009. The Potential to Narrow Uncertainty in Regional Climate
591 Predictions. B. Am. Meteorol. Soc., 90(8), 1095–1107.

592 Heldal, H. E., I. Stupakoff and N. S. Fisher, 2001. Bioaccumulation of 137-Cs and 57-Co by
593 five marine phytoplankton species. J. Environ. Radioactiv., 57, 231-236.

594 IAEA, International Atomic Energy Agency, 2004. Sediment Distribution Coefficients and
595 Concentration Factors for Biota in the Marine Environment. IAEA, Vienna.

596 Kanda, J., 2013. Continuing 137-Cs release to the sea from the Fukushima Dai-ichi Nuclear
597 Power Plant through 2012, Biogeosciences Discuss., 10, 3577-3595.

598 Kawamura H, T. Kobayashi, A. Furuno, T. In, Y. Ishikawa, T. Nakayama, S. Shima and T.
599 Awaji, 2011. Preliminary numerical experiments on oceanic dispersion of 131I and 137Cs
600 discharged into the ocean because of Fukushima Daiichi nuclear power plant disaster, J.
601 Nucl. Sci. Technol., 48, 1349-1356.

602 Kobayashi, T., S. Otosaka, O. Togawa and K. Hayashi, 2007. Development of a Non-
603 conservative Radionuclides Dispersion Model in the Ocean and its Application to Surface
604 Cesium-137 Dispersion in the Irish Sea, J. Nucl. Sci. Technol., 44:2, 238-247.

605 Kusakabe, M., S. Oikawa, H. Takata, and J. Misonoo, 2013. Spatio-temporal distributions of
606 Fukushima-derived radionuclides in surface sediments in the waters off Miyagi, Fukushima,
607 and Ibaraki Prefectures, Japan. Biogeosciences Discuss., 10, 4819-4850.

608 Livingston, H. D., P. P. Povinec, 2000. Anthropogenic marine radioactivity, Ocean Coast.
609 Manage., 43, 689-712.

610 Masumoto et al., 2004. A Fifty-Year Eddy-Resolving Simulation of the World Ocean -
611 Preliminary Outcomes of OFES (OGCM for the Earth Simulator), J. Earth Simulator, vol 1, p
612 35-56.

613 Monte L., R. Perianez, P. Boyer, J.T. Smith and J.E. Brittain, 2009. The role of physical
614 processes controlling the behaviour of radionuclide contaminants in the aquatic environment:
615 a review of state-of-the-art modelling approaches. J. Environ. Radioactiv., 100, 779-784.25.

616 Nagao, S., M. Kanamori, S. Ochiai, S. Tomihara, K. Fukushi and M. Yamamoto, 2013.
617 Export of 134-Cs and 137-Cs in the Fukushima river systems at heavy rains by Typhoon
618 Roke in September 2011, Biogeosciences Discuss., 10, 2767-2790.

619 Nakano, H., T. Motoi, K. Hirose, and M. Aoyama, 2010. Analysis of 137Cs concentration in
620 the Pacific using a Lagrangian approach, J. Geophys. Res., 115, C06015.

621 Nakano M. and P.P. Povinec, 2012. Long-term simulations of the 137-Cs dispersion from the
622 Fukushima accident in the world ocean, J. Environ. Radioac., 111, 109-115.

623 Niiler, P.P., N.A. Maximenko, G.G. Panteleev, T. Yamagata, and D.B. Olson, 2003. Near-
624 surface dynamical structure of the Kuroshio Extension, J. Geophys. Res., 108, C63193.

625 Nonaka, M., S-P Xie and H. Sasaki, 2012. Interannual variations in low potential vorticity
626 water and the subtropical countercurrent in an eddy-resolving OGCM, J. Oceanogr., 68, p
627 139-150.

628 Normile, D., The Pacific Swallows Fukushima's Fallout, 2013. Science, 340, 6132, 547,
629 doi10.1126/science.340.6132.547.

630 Oka E. and B.Qiu, 2011. Progress of North Pacific mode water research in the past decade. J.
631 Oceanogr. doi 10.1007/s10872-011-0032-5.

632 Paris C.B., J. Helgers, E. Van Sebille and A. Srinivasan, 2013. The Connectivity Modeling
633 System: A probabilistic modelling tool for the multi-scale tracking of biotic and abiotic
634 variability in the ocean. Environ. Modell. Softw. in press.

635 Periañez, R., 2000. Modelling the tidal dispersion of 137-Cs and 239,240-Pu in the English
636 Channel, Journal of Environmental Radioactivity 49, 259-277.

637 Periañez, R. and A.J. Elliott, 2002. A particle-tracking method for simulating the dispersion
638 of non-conservative radionuclides in coastal waters. J. Environ. Radioac. 58, 13-33.

639 Qiu, B., and S. Chen, 2005. Variability of the Kuroshio Extension jet, recirculation gyre and
640 mesoscale eddies on decadal timescales, J. Phys. Oceanogr., 35, 2090-2103.

641 Qu, T., and J. Chen, 2009. A North Pacific decadal variability in subduction rate, Geophys.
642 Res. Lett, 36 (22), L22602, doi:10.1029/2009GL040914.

643 Rossi, V., C. Lopez, E. Hernandez-Garcia, J. Sudre, V. Garcon and Y. Morel, 2009. Surface
644 mixing and biological activity in the four Eastern Boundary Upwelling Systems, Nonlin.
645 Processes Geophys., 16, 557–568.

646 Sasaki H., Nonaka M., Masumoto Y., Sasai Y., Uehara H. and H. Sakuma, 2008. An eddy-
647 resolving hindcast simulation of the quasiglobal ocean from 1950 to 2003 on the Earth
648 Simulator. In: Hamilton K., Ohfuchi W. (eds) High resolution numerical modelling of the
649 Atmosphere and Ocean. Springer, New York, p 157–185.

650 Sasaki, H., S-P Xie, B. Taguchi, M. Nonaka, S. Hosoda and Y. Masumoto, 2012. Interannual
651 variations of the Hawaiian Lee Countercurrent induced by potential vorticity variability in the
652 subsurface, J. Oceanogr., 68, p 93-111.

653 Stohl A., P. Seibert, G. Wotawa, D. Arnold, J.F. Burkhart, S. Eckhardt, C. Tapia, A. Vargas,
654 and T. J. Yasunari, 2011. Xenon-133 and caesium-137 releases into the atmosphere from the
655 Fukushima Dai-ichi nuclear power plant: determination of the source term, atmospheric
656 dispersion, and deposition. Atmos. Chem. Phys. Discuss., 11, 28319-28394.

657 Taguchi B., S-P. Xie, N. Schneider, M. Nonaka, H. Sasaki and Y. Sasai, 2007. Decadal
658 Variability of the Kuroshio Extension: Observations and an Eddy-Resolving Model Hindcast.
659 J. Clim, 20(11), 2357-2377.

660 Taguchi B., B. Qiu, M. Nonaka, H. Sasaki, S-P. Xie and N. Schneider, 2010. Decadal
661 variability of the Kuroshio Extension: mesoscale eddies and recirculations, Ocean Dynam.,
662 vol 60, p. 673–691.

663 Tsumune, D., M. Aoyama, K. Hirose, F.O. Bryan, K. Lindsay, G. Danabasoglu, 2011.
664 Transport of 137Cs to the Southern Hemisphere in an ocean general circulation model, Prog.
665 Oceanogr., 89, 38-48.

666 Tsumune D., T. Tsubono, M. Aoyama and K. Hirose, 2012. Distribution of oceanic 137-Cs
667 from the Fukushima Dai-ichi nuclear power plant simulated numerically by a regional ocean
668 model. J. Environ. Radioact., 111, 100–108, 10.1016/j.jenvrad.2011.10.007.

669 Tsumune, D., T. Tsubono, M. Aoyama, M. Uematsu, K. Misumi, Y. Maeda, Y. Yoshida, and
670 H. Hayami, 2013. One-year, regional-scale simulation of 137Cs radioactivity in the ocean
671 following the Fukushima Daiichi Nuclear Power Plant accident, Biogeosciences Discuss., 10,
672 6259-6314.

673 Van Sebille, E., 2009. Assessing Agulhas leakage, PhD dissertation, Utrecht University.

674 Van Sebille, E., M.O. Baringer, W.E. Johns, C.S. Meinen, L.M. Beal, F. de Jong and H.M.
675 van Aken (2011), Propagation pathways of classical Labrador Sea Water from its source
676 region to 26˚N, J. Geophys. Res., 116, C12027.

677 Van Sebille, E., W.E. Johns and L.M. Beal, 2012. Does the vorticity flux from Agulhas rings
678 control the zonal pathway of NADW across the South Atlantic? J. Geophys. Res., 117,
679 C05037.

680 Vogel C. and N. S. Fisher, 2010. Metal accumulation by heterotrophic marine
681 bacterioplankton. Limnol. Oceanogr., 55(2), 519-528.

682 Yasunari T.J., A. Stohl, R.S. Hayano, J.F. Burkhart, S. Eckhardt, and T. Yasunari, 2011.
683 Cesium-137 deposition and contamination of Japanese soils due to the Fukushima nuclear
684 accident. Proc. Natl. Acad. Sci. USA, 108, 49, 19530-19534.

685

686 **Figure captions**

687

688 **Figure 1:** Surface (0-200m) Cs-137 concentrations (Bq/m^3). a) In April 2012, b) April 2014
689 c) April 2016, d) April 2021 and e) along 37.5°N at the latitude of Fukushima plant (black
690 dashed line in panels a-d). Error bars in e) represent the standard deviation over the ensemble
691 of 27 simulations. The black square around the Hawaii archipelago and the black line along
692 the North American west coast represent our areas of interest. White flow vectors represent
693 an illustrative sense of the large-scale surface circulation at various locations.

694

695 **Figure 2:** Surface (0-200 m) Cs-137 concentrations (Bq/m^3) along selected continental
696 shelves. a) Hovmöller diagram (latitude versus time) of Cs-137 concentrations (Bq/m^3) along
697 the North American western continental shelves (concentrations are averaged over a ~300 km
698 wide coastal band as shown by the black line in Fig. 1. b) Cs-137 concentrations at 30°N,
699 49°N (indicated by the two dotted white lines on panel a) and around the Hawaii archipelago
700 (see the black square in Fig. 1a, b, c, d), error bars representing the standard deviation over
701 the ensemble simulations.

702

703 **Figure 3:** Vertical distribution of Cs-137 over time in the North Pacific basin. "Surface"
704 waters are defined from 0 to 200 m, "Central" from 200 to 600 m, "Intermediate" from 600 to
705 1500 m and "Deep" below 1500 m. Percentage is given over the total remaining part of Cs-
706 137, taking into account its natural decay.

707

708 **Figure 4:** a) Subsurface (400-600 m) Cs-137 concentrations (Bq/m^3) in April 2014. b, c, d)
709 Vertical sections of Cs-137 concentrations (Bq/m^3) in April 2014 at 30°N (b), along 165°E
710 (c) and 140°W (d). Black contours in a) represent the mean depth (in m) of the σ_0 = 26 kg/m^3

711 isopycnal, while the mean stratification is shown in b, c, and d, as derived from the OFES
712 ensemble. The white dotted lines indicate the position of the respective sections.
713
714 **Figure 5:** Subsurface concentrations of Cs-137 (Bq/m^3) in April 2021 a) at 400-600 m and b)
715 at 150-250 m and c) along a vertical section at 30°N (white dotted rectangles show the
716 horizontal sections in a, b). Black contours in b) represent the annual mean depth (in m) of
717 the σ_0 = 26 kg/m^3, isopycnal, as derived from the OFES ensemble. The white dotted lines
718 indicate the position of the respective sections.
719
720 **Figure 6:** Original depth (m) of upwelled particles 1 year before reaching the surface shelf
721 waters within the two black boxes at the coast represented in panel 5b) (28-30°N and 48-
722 50°N). Bars are the ensemble mean distributions, error lines indicate the standard deviation of
723 the distributions as obtained from the 27 ensemble members.
724

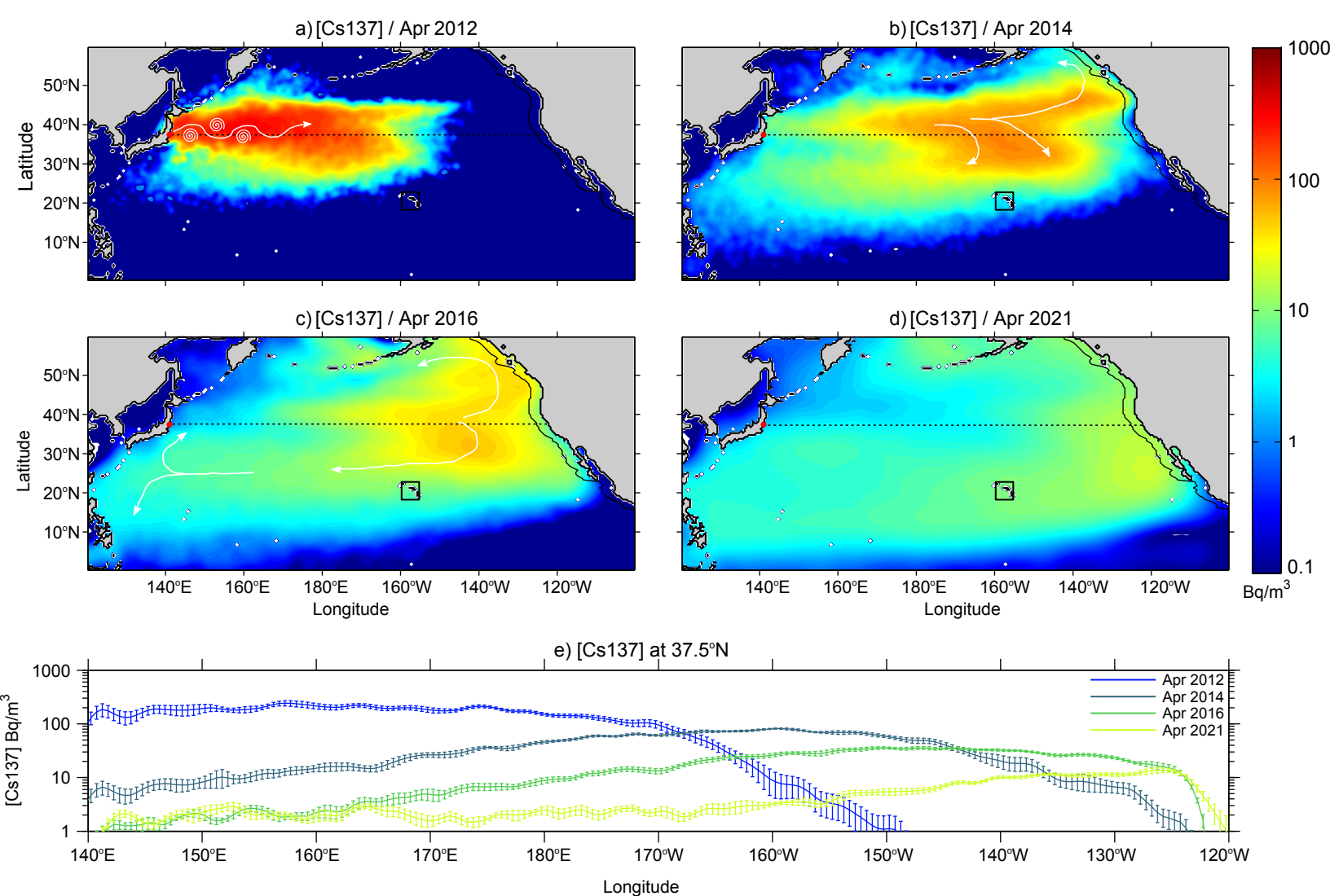
a) [Cs137] / Apr 2012
b) [Cs137] / Apr 2014
c) [Cs137] / Apr 2016
d) [Cs137] / Apr 2021
Latitude
50°N
40°N
30°N
20°N
10°N
140°E
160°E
180°E
160°W
140°W
120°W
Longitude
1000
100
10
1
0.1
Bq/m3
e) [Cs137] at 37.5°N
[Cs137] Bq/m3
150°E
170°E
170°W
150°W
130°W
Apr 2012
Apr 2014
Apr 2016
Apr 2021

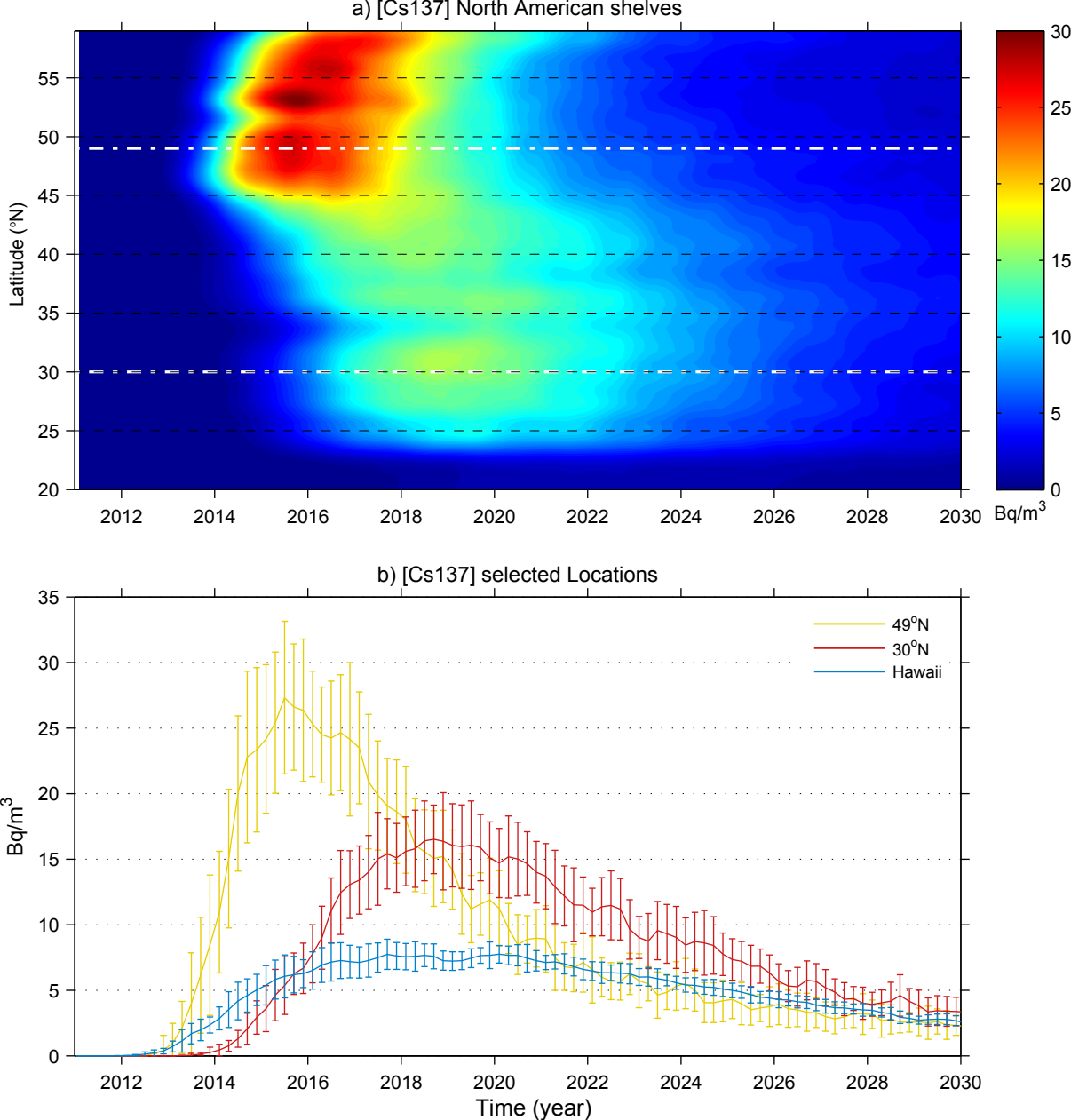
a) [Cs137] North American shelves
Latitude (°N)
55
50
45
40
35
30
25
20
2012
2014
2016
2018
2020
2022
2024
2026
2028
2030
30
25
20
15
10
5
0
Bq/m3
b) [Cs137] selected Locations
Bq/m3
35
30
25
20
15
10
5
0
49°N
30°N
Hawaii
2012
2014
2016
2018
2020
2022
2024
2026
2028
2030
Time (year)

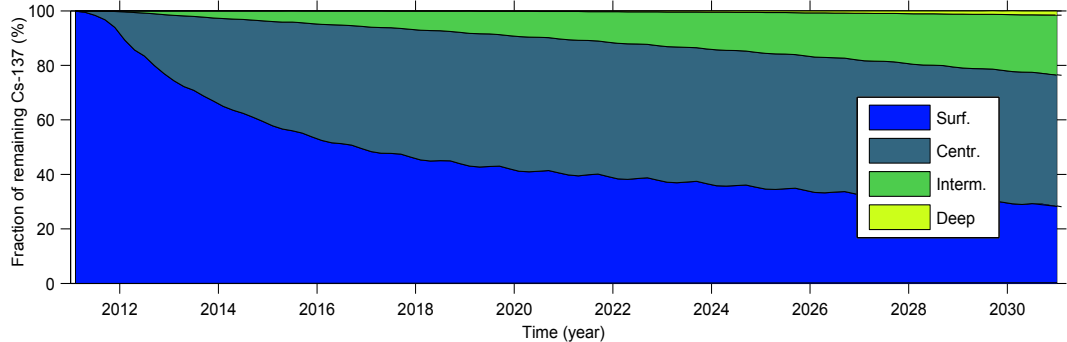
Fraction of remaining Cs-137 (%)
100
80
60
40
20
0
2012
2014
2016
2018
2020
2022
2024
2026
2028
2030
Time (year)
Surf.
Centr.
Interm.
Deep

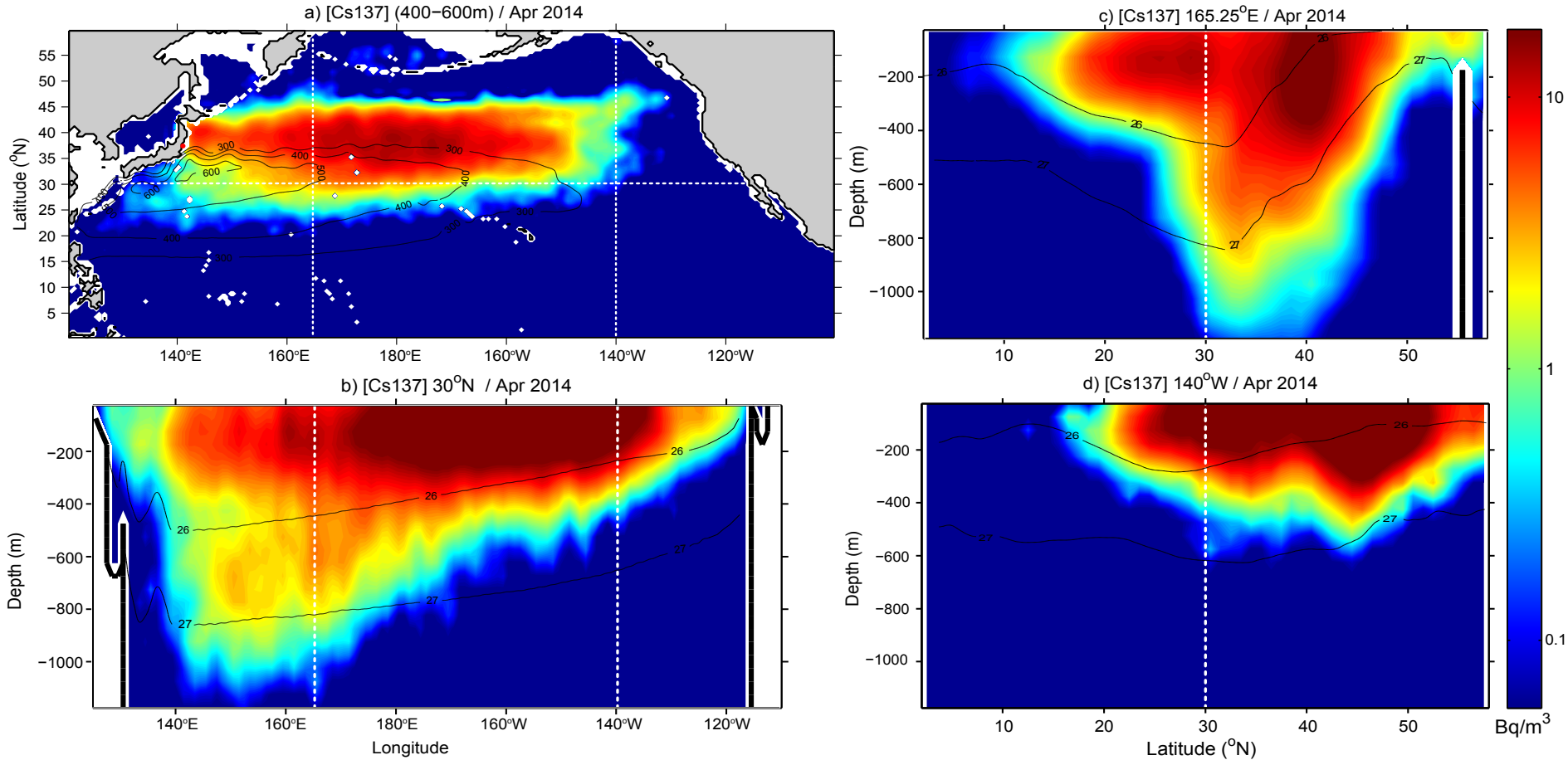
a) [Cs137] (400−600m) / Apr 2014
Latitude (°N)
55
50
45
40
35
30
25
20
15
10
5
140°E
160°E
180°E
160°W
140°W
120°W
300
400
500
600
c) [Cs137] 165.25°E / Apr 2014
Depth (m)
−200
−400
−600
−800
−1000
10
20
30
40
50
25
26
27
b) [Cs137] 30°N / Apr 2014
Depth (m)
Longitude
d) [Cs137] 140°W / Apr 2014
Depth (m)
Latitude (°N)
10
1
0.1
Bq/m3

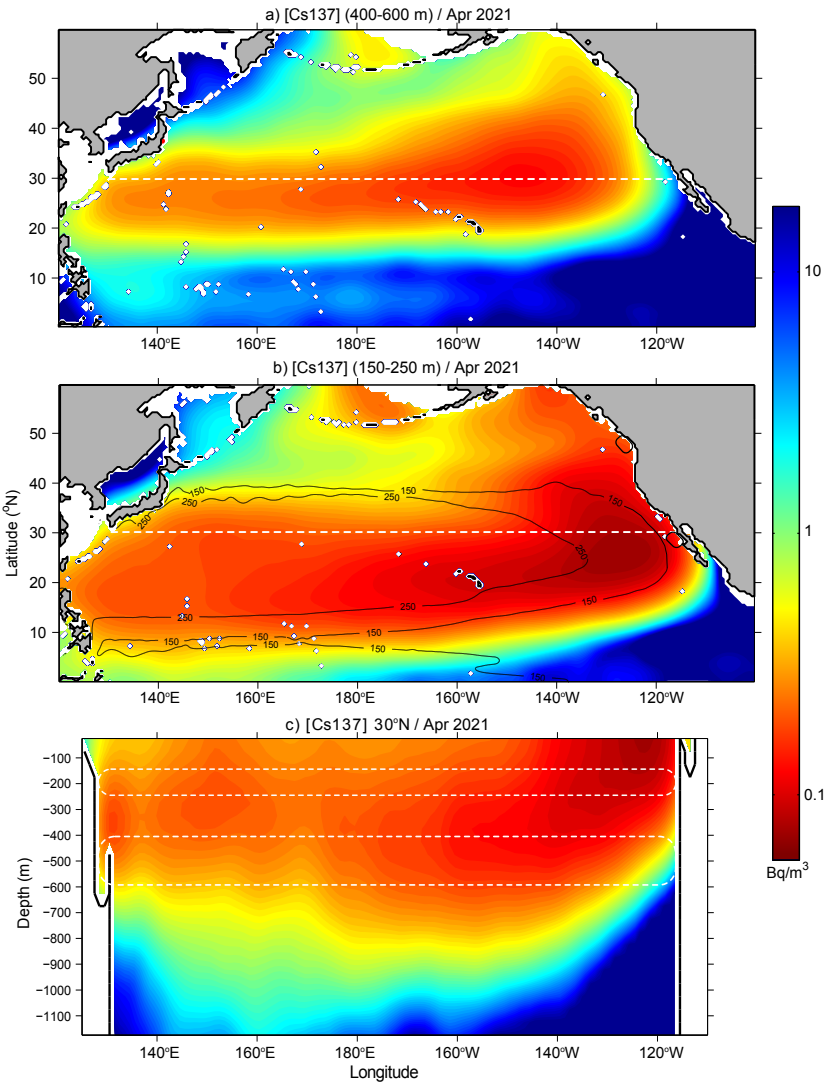
a) [Cs137] (400-600 m) / Apr 2021
b) [Cs137] (150-250 m) / Apr 2021
c) [Cs137] 30°N / Apr 2021
Latitude (°N)
Depth (m)
Longitude
140°E
160°E
180°E
160°W
140°W
120°W
Bq/m3
10
1
0.1

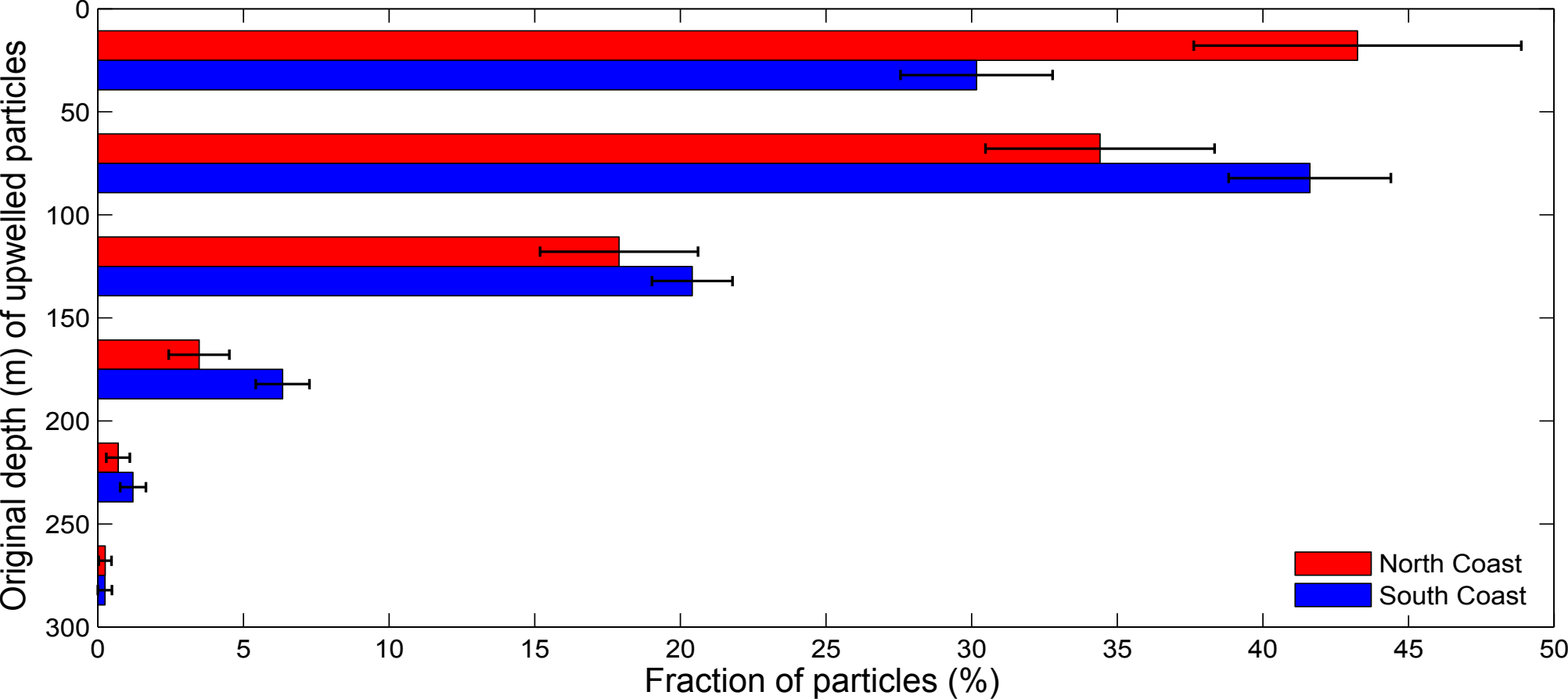
Original depth (m) of upwelled particles
0
50
100
150
200
250
300
0
5
10
15
20
25
30
35
40
45
50
Fraction of particles (%)
North Coast
South Coast